Swing-up of an Inverted Pendulum on a Cart Using a Modified Energy Based Approach

Emese Kennedy, and Hien Tran, *Member, SIAM*

Abstract—In this paper, we present a modified energy-based swing-up controller for a single inverted pendulum (SIP) on a cart. The controller was derived using a more complex dynamical model for the SIP system than models that are commonly used. We also consider the effects of viscous damping, and incorporate physical restrictions like the maximum deliverable voltage by the amplifier, the capacity of the DC motor that drives the cart, as well as the finite track length.

Index Terms—inverted pendulum, real-time implementation, energy-based control, swing-up, Lyapunov function.

I. Introduction

The control of an inverted pendulum is considered a benchmark problem in nonlinear control theory. Because of its popularity and numerous applications, there are many existing control methods for both the swing-up and the stabilization of the inverted pendulum. However, many of the published controllers have only been tested in simulations and not in real-time experiments [1]. Comparing experimental results with published work of others, the simulation results are often different from the real-time results. This is because almost all simulations use a simplified model to represent the dynamics of the inverted pendulum. Furthermore, most of the simulations ignore the effects of friction, and often fail to incorporate some physical restrictions like the maximum deliverable voltage by the amplifier, the capacity of the DC motor that drives the cart, and the finite track length [2].

II. System Dynamics

A. Conventions

Figure 1 shows a diagram of the Single Inverted Pendulum (SIP) mounted on a linear cart. We define the positive sense of rotation counterclockwise, when facing the cart. The perfectly upright position of the pendulum corresponds to the zero angle, modulus 2π, (i.e. $\alpha = 0$ rad $[2\pi]$). The positive direction of the cart's displacement is to the right when facing the cart.

B. System Parameters

The model parameters and their values as specified by Quanser in [3] and [4] are provided in Table I.
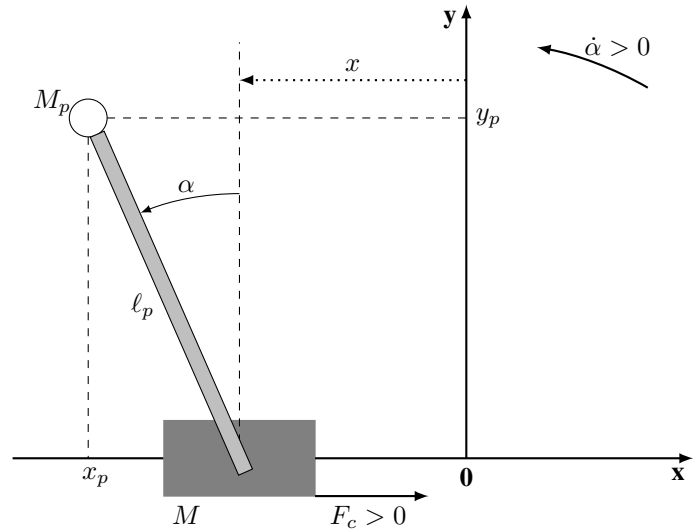
Fig. 1. Single inverted pendulum diagram.

TABLE I
INVERTED PENDULUM MODEL PARAMETERS

Symbol	Description	Value
M_w	Cart Weight Mass	0.37 kg
M	Cart Mass with Extra Weight	$0.57 + M_w$ kg
J_m	Rotor Moment of Inertia	3.90E-007 kg.m^2
K_g	Planetary Gearbox Gear Ratio	3.71
r_{mp}	Motor Pinion Radius	6.35E-003 m
B_{eq}	Equivalent Viscous Damping Coefficient	5.4 N.m.s/rad
M_p	Pendulum Mass	0.230 kg
ℓ_p	Pendulum Length from Pivot to COG	0.3302 m
I_p	Pendulum Moment of Inertia about its COG	7.88E-003 kg.m^2
B_p	Viscous Damping Coefficient	0.0024 N.m.s/rad
g	Gravitational Constant	9.81 m/s^2
K_t	Motor Torque Constant	0.00767 N.m/A
K_m	Back-ElectroMotive-Force Constant	0.00767 V.s/rad
R_m	Motor Armature Resistance	2.6 Ω

C. Equations of Motion

The dynamic model for the system can be derived using Lagrange's method. For this method, we treat the driving force, F_c, generated by the DC motor acting on the cart through the motor pinion as the single input to the system. As we showed in [5] and [2], the second-order time derivatives of x and α are the two nonlinear equations

$$
\ddot{x} = \Bigg(-(I_p + M_p\ell_p^2)B_{eq}\dot{x} - M_p\ell_p\cos(\alpha)B_p\dot{\alpha}
$$
$$
- (M_p^2\ell_p^3 + I_pM_p\ell_p)\sin(\alpha)\dot{\alpha}^2 + (I_p + M_p\ell_p^2)F_c \quad (1)
$$
$$
+ M_p^2\ell_p^2 g\cos(\alpha)\sin(\alpha) \Bigg) \Bigg/ D(\alpha)
$$

and

$$\ddot{\alpha} = \left((M + M_p)M_p g \ell_p \sin(\alpha) - (M + M_p)B_p\,(\dot{\alpha}) \right.$$
$$- M_p^2 \ell_p^2 \sin(\alpha)\cos(\alpha)\,(\dot{\alpha})^2 - M_p \ell_p \cos(\alpha)B_{eq}\,(\dot{x}) \quad (2)$$
$$\left. + M_p \ell_p \cos(\alpha)F_c \right) \Big/ D(\alpha),$$

where $D(\alpha) = (M + M_p)I_p + MM_p\ell_p^2 + M_p^2\ell_p^2\sin^2(\alpha)$, and x and α are both functions of t. Equations (1) and (2) represent the equations of motion (EOM) of the system.

In our implementation the system's input is equal to the cart's DC motor voltage, V_m, so we must convert the driving force, F_c, to voltage input. Using Kirchhoff's voltage law and the physical properties of our system, it can be shown that

$$F_c = -\frac{K_g^2 K_t K_m\,(\dot{x}(t))}{R_m r_{mp}^2} + \frac{K_g K_t V_m}{R_m r_{mp}}. \quad (3)$$

III. ENERGY-BASED CONTROLLER

A. Pendulum's Energy

One of the most popular control methods for swinging up the pendulum is where the control law is chosen such that the energy of the pendulum builds until reaching the upright equilibrium. This technique was first proposed and implemented by Astrom and Furuta [6], [7]. Here, we present a modified approach based on a more complex dynamical model for the SIP system than the simplified model that is most commonly used. We also consider the electrodynamics of the DC motor that drives the cart, incorporate viscous damping friction as seen at the motor pinion, and account for the limitation of having a cart-pendulum system with a finite track length.

The total energy, $\mathcal{E}_p$, of the pendulum at it's hinge is given by the sum of it's rotational kinetic energy and it's potential energy, so

$$\mathcal{E}_p = \frac{1}{2}J_p\dot{\alpha}^2 + M_p\ell_p g(\cos(\alpha) - 1), \quad (4)$$

where J_p, the pendulum's moment of inertia at it's hinge, is defined as

$$J_p = \int_0^{2\ell_p} r^2 \frac{M_p}{2\ell_p} dr = \frac{4}{3}M_p\ell_p^2. \quad (5)$$

Since our goal is to increase the energy of the pendulum until the upright position is reach, we must design a controller so that the condition

$$\frac{d\mathcal{E}_p}{dt} \geq 0 \quad (6)$$

is guaranteed. By differentiating (4) we have

$$\frac{d\mathcal{E}_p}{dt} = J_p\dot{\alpha}\ddot{\alpha} - M_p\ell_p g \sin(\alpha)\dot{\alpha}$$
$$= \frac{4}{3}M_p\ell_p^2\dot{\alpha}\ddot{\alpha} - M_p\ell_p g \sin(\alpha)\dot{\alpha}. \quad (7)$$

B. Lagrange's Equations

The Lagrangian, $\mathcal{L}$, is given by

$$\mathcal{L} = \mathcal{K}_T - \mathcal{V}_T, \quad (8)$$

where

$$\mathcal{K}_T = \frac{1}{2}\left(M + M_p + \frac{J_m K_g^2}{r_{mp}^2}\right)\dot{x}(t)^2 + \frac{2}{3}M_p\ell_p^2\dot{\alpha}(t)^2$$
$$- M_p\ell_p\cos(\alpha(t))\dot{x}(t)\dot{\alpha}(t) \quad (9)$$

is the total kinetic energy, and

$$\mathcal{V}_T = M_p g y_p = M_p g \ell_p \cos(\alpha(t)) \quad (10)$$

is the total potential energy [2]. By definition, the two Lagrange's equations for our system are

$$\frac{\partial^2}{\partial t \partial \dot{x}}\mathcal{L} - \frac{\partial}{\partial x}\mathcal{L} = F_c - B_{eq}\dot{x}(t) \quad (11)$$

and

$$\frac{\partial^2}{\partial t \partial \dot{\alpha}}\mathcal{L} - \frac{\partial}{\partial \alpha}\mathcal{L} = -B_p\dot{\alpha}(t), \quad (12)$$

where B_{eq} is the equivalent viscous damping coefficient as seen at the motor pinion, and B_p is the equivalent viscous damping coefficient as seen at the pendulum axis. Thus, equations (11) and (12) account for friction in the form of equivalent viscous damping, however, it should be noted that in the development of the current model the (nonlinear) Coulomb friction applied to the cart, and the force on the cart due to the pendulum's action have been neglected. Equation (11) can be rewritten as

$$\left(M + M_p + \frac{J_m K_g^2}{r_{mp}^2}\right)\ddot{x}(t) + M_p\ell_p\sin(\alpha(t))\dot{\alpha}(t)^2$$
$$- M_p\ell_p\cos(\alpha(t))\ddot{\alpha}(t) = F_c - B_{eq}\dot{x}(t), \quad (13)$$

and (12) can be rewritten as

$$-M_p\ell_p\cos(\alpha(t))\ddot{x}(t) + \frac{4}{3}M_p\ell_p^2\ddot{\alpha}(t) - M_p\ell_p g \sin(\alpha(t))$$
$$= -B_p\dot{\alpha}(t). \quad (14)$$

Then, by using (14), equation (7) becomes

$$\frac{d\mathcal{E}_p}{dt} = M_p\ell_p\dot{\alpha}\cos(\alpha)\ddot{x} - B_p\dot{\alpha}^2. \quad (15)$$

Using Newton's second law of motion together with D'Alemberts principle, we can express (15) as

$$\frac{d\mathcal{E}_p}{dt} = M_p\ell_p\dot{\alpha}\cos(\alpha)\left(\frac{K_g K_t r_{mp} V_m}{R_m(M r_{mp}^2 + K_g^2 J_m)}\right.$$
$$\left. - \frac{(K_g^2 K_t K_m + B_{eq} R_m r_{mp}^2)\dot{x}}{R_m(M r_{mp}^2 + K_g^2 J_m)}\right) - B_p\dot{\alpha}^2. \quad (16)$$

C. Lyapunov Stability Condition

Consider the Lyapunov function

$$L(X) = \frac{1}{2}\mathcal{E}_p^2 + k(1 - \cos^3(\alpha)), \quad (17)$$

where k is a positive constant. Equation (17) only has one zero, namely the upright position with zero angular velocity (i.e. $\alpha = 0, \dot{\alpha} = 0$), and is strictly positive everywhere else.
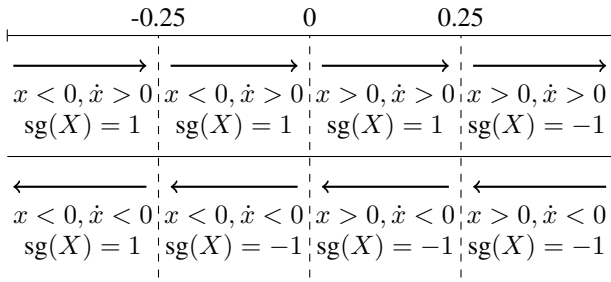
Fig. 2. Diagram representing how sg(X) is defined. The arrows indicate the direction of the cart's displacement, while the number line indicates the cart's position.

Then, based on Lyapunovs theorem, our control input, V_m, must satisfy

$$\frac{dL}{dt} = \mathcal{E}_p M_p \ell_p \dot{\alpha} \cos(\alpha) \left(\frac{K_g K_t r_{mp} V_m}{R_m(Mr_{mp}^2 + K_g^2 J_m)} \right.$$
$$\left. - \frac{(K_g^2 K_t K_m + B_{eq} R_m r_{mp}^2)\dot{x}}{R_m(Mr_{mp}^2 + K_g^2 J_m)} \right)$$
$$+ \frac{3}{2}k\cos(\alpha)\sin(2\alpha)\dot{\alpha} - \mathcal{E}_p B_p \dot{\alpha}^2$$
$$\leq 0. \tag{18}$$

Substituting the model parameter values provided in Table I into (18), and simplifying yields the condition

$$\mathcal{E}_p \dot{\alpha} \cos(\alpha)(V_m - 7.614\dot{x})$$
$$+ 12.28k\dot{\alpha}\cos(\alpha)\sin(2\alpha) - 0.0197\mathcal{E}_p\dot{\alpha}^2$$
$$\leq 0, \tag{19}$$

that our swing-up controller must satisfy to guarantee Lyapunov stability.

D. Control Law

Consider the control law of the form

$$V_m(X) = \beta_1|\dot{x}|\left(-\beta_2\text{sign}(\mathcal{E}_p\dot{\alpha}\cos(\alpha)) + \text{sg}(X)e^{\eta|x|} \right)$$
$$- \frac{\beta_3\text{sign}(\dot{\alpha}\cos(\alpha))|\sin(2\alpha)|}{\mathcal{E}_p}$$
$$+ 0.0197\text{sign}(\mathcal{E}_p)\dot{\alpha}\cos\alpha, \tag{20}$$

where β_1, β_3, η, and $0 < \beta_2 < 1$ are positive constants, and the function sg(X) is defined as

$$\text{sg}(X) = 0.5(\text{sign}(\dot{x}) - \text{sign}(x)$$
$$- \text{sign}(|x| - 0.25)(\text{sign}(\dot{x}) + \text{sign}(x))), \tag{21}$$

which will output ± 1 depending on the position of the cart and the direction it is moving. The total length of the track that the cart can travel is 0.814 m, indicating that the cart's horizontal displacement in either direction must be less than 0.407 m (i.e. $|x| < 0.407$ m). For safety reasons, the cart should not get too close to the end of the track, thus sg(X) was defined in such a way that it switches signs only when the cart's displacement from the center is more than 0.25 m and the direction of the cart's displacement is towards either track end. Figure 2 represents how sg(X) is defined. Substituting (20) into (19), and simplifying results in

$$\mathcal{E}_p\dot{\alpha}\cos(\alpha)\left(\beta_1|\dot{x}|\left(-\beta_2\text{sign}(\mathcal{E}_p\dot{\alpha}\cos(\alpha)) + \text{sg}(X)e^{\eta|x|}\right)\right.$$
$$\left. -7.614\dot{x}\right) - \beta_3|\dot{\alpha}\cos(\alpha)||\sin(2\alpha)|$$
$$+ 12.28k\dot{\alpha}\cos(\alpha)\sin(2\alpha) - 0.0197\sin^2(\alpha)|\mathcal{E}_p|\dot{\alpha}^2$$
$$\leq 0. \tag{22}$$

It can be shown that (22) is satisfied when

$$\frac{7.614}{e^{\eta|x|} + \beta_2} \leq \beta_1 \leq \frac{7.614}{e^{\eta|x|} - \beta_2}, \tag{23}$$

and $\beta_3 \geq 12.28k$ [2]. Physically for our system, a positive input voltage means positive cart displacement, therefore V_m and $\dot{x}$ have the same sign. This means that the sign of V_m should be given by the value of sg(X) to make sure the cart avoids the edges of the track. Therefore, we must have

$$\text{sign}\left(\beta_1|\dot{x}|\left(-\beta_2\text{sign}(\mathcal{E}_p\dot{\alpha}\cos(\alpha)) + \text{sg}(X)e^{\eta|x|}\right)\right.$$
$$\left. - \frac{\beta_3\text{sign}(\dot{\alpha}\cos(\alpha))|\sin(2\alpha)|}{\mathcal{E}_p}\right) \tag{24}$$
$$= \text{sg}(X).$$

Considering the possible sign combinations [2], we can show that (24) holds when the constants $\beta_1, \beta_2, \beta_3$, and η satisfy

$$\beta_1 > \frac{\beta_3|\sin(2\alpha)|}{|\dot{x}||\mathcal{E}_p|(e^{\eta|x|} - \beta_2)}. \tag{25}$$

To avoid division by zero and bound the value of β_1, we can saturate the signals of $\mathcal{E}_p$ and $\dot{x}$ so that $|\mathcal{E}_p| > \delta_1$ and $|\dot{x}| > \delta_2$ for some small positive constants δ_1 and δ_2. Then, the condition (25) will be satisfied when

$$\beta_1 \geq \frac{\beta_3}{\delta_1\delta_2(1 - \beta_2)}. \tag{26}$$

Moreover, we must ensure that the amplifier doesn't go into saturation (i.e. $|V_m| \leq 10$). The choice of the constants in the control law that satisfy all the restrictions is somewhat arbitrary. A particular choice of constants that will satisfy all conditions for the controller in (20), taking into account that the maximum value for $\dot{x}$ is 1.075 m/s, is $\beta_1 = 4.8$, $\beta_2 = 0.6$, $\beta_3 = 0.0115$, and $\eta = 0.6$. These constants were calculated using $k = 10^{-4}$, $\delta_1 = 0.001$, and $\delta_2 = 0.1$.

IV. REAL-TIME IMPLEMENTATION

A. Apparatus

For our real-time experiments we use apparatus designed and provided by Quanser Consulting Inc. (119 Spy Court Markham, Ontario, L3R 5H6, Canada). This includes a single inverted pendulum mounted on an IP02 servo plant (pictured in Figure 3), a VoltPAQ amplifier, and a Q2-USB DAQ control board. The IP02 cart incorporates a Faulhaber Coreless DC Motor (2338S006) coupled with a Faulhaber Planetary Gearhead Series 23/1. The cart is also equipped with a US Digital S1 single-ended optical shaft encoder. The detailed technical specifications can be found in [3]. A diagram of our experimental setup is included in Figure 4.
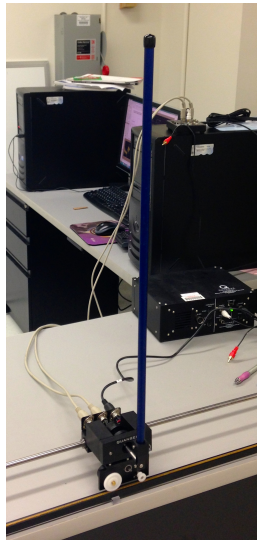
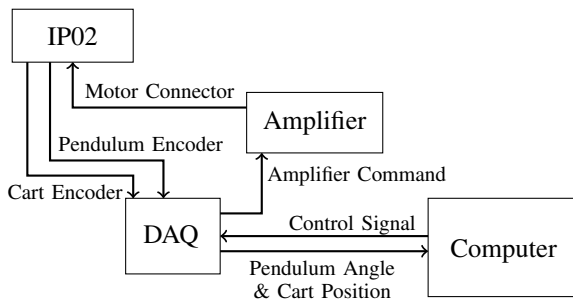Fig. 3.   Single inverted pendulum mounted on a Quanser IP02 servo plant.

Fig. 4.   Diagram of experimental setup.

B. Simulation Results

The controller given by (20) was tested in simulation with $\beta_1 = 4.8$, $\beta_2 = 0.6$, $\beta_3 = 0.0115$, and $\eta = 0.6$, using MATLAB Simulink. Since the starting downward position of the pendulum is a stable equilibrium we must input some initial voltage to get the experiment started. The starting voltage for our simulation was 8 Volts that was applied for 0.1 second. The state responses and the corresponding control effort are depicted in Figures 5 and 6. The dashed blue lines in the second graph in 5(b) indicate the region where the stabilization control can take over (i.e. where $|\alpha| < 15°$). The simulation indicates that the controller swings the pendulum up into the upright position in approximately 30 seconds. Furthermore, all the values of the states and the required control effort stayed within the possible ranges deliverable by the apparatus we use for real time experiments. Figure 5(a) also indicates that the cart did not go past the end of the track.

C. Experimental Results

The swing-up controller given by (20) was successfully implemented in real-time with $\beta_1 = 4.8$, $\beta_2 = 0.6$, $\beta_3 = 0.0115$, and $\eta = 0.6$ using MATLAB Simulink. The state responses and the corresponding control effort are shown in Figures 7 and 8. Figure 7(b) indicates that the controller swung up the pendulum in approximately 15 seconds. On one occasion the required control effort reached the upper limit of 10 Volts and had to be saturated. The

average amount of voltage used during the experiment was about 2.89 Volts. Once the pendulum reached within $15°$ of the upright position, the power series based stabilization controller presented in [5] successfully took over [2].

The experiment was repeated several times with swing-up times ranging between 15 and 40 seconds. During the swing-up procedure the cart makes very fast big moves because of how the function sg is defined. When the cart moves close to the end of the track, the controller successfully makes the cart moving away from the edge, but this action results in a jerk of the cart. Unfortunately, sometimes when the pendulum is near the upright position, this fast jerk of the cart overpowers the movement of the pendulum and makes the pendulum loose momentum. When this happens, making up the loss of momentum increases the swing-up time [2].

V. conclusion

We presented a controller based on the work of Astrom and Furuta [6], [7] to create a new energy-based swing-up method that was derived using a more complex dynamical model for the SIP system than the simplified models that are commonly used. It is often the case, that a controller based on a simplified model works well in simulation, but not in real-time. For the purposes of real-time implementation and many applications, it is desirable to consider the effects of friction, and incorporate physical restrictions of the SIP system like the maximum deliverable voltage by the amplifier, the capacity of the DC motor that drives the cart, and the finite track length. The control method presented accounts for viscous damping friction, and it also takes many of the physical restrictions of the actual SIP system into account. Even though the controller can successfully swing-up the pendulum, the amount of time it takes for the pendulum to reach the upright position varies between 15 and 40 seconds [2].

References

[1] O. Boubaker, "The inverted pendulum benchmark in nonlinear control theory: A survey," *International Journal of Advanced Robotic Systems*, vol. 10, pp. 1–9, 2013.

[2] E. Kennedy, "Swing-up and stabilization of a single inverted pendulum: Real-time implementation," Ph.D. dissertation, North Carolina State University, 2015. [Online]. Available: http://www.lib.ncsu.edu/resolver/1840.16/10416

[3] *Linear Motion Servo Plants: IP01 or IP02 - IP01 and IP02 User Manual*, 5th ed., Quanser Consulting, Inc.

[4] *Linear Motion Servo Plants: IP01 or IP02 - Single Inverted Pendulum (SIP) User Manual*, 3rd ed., Quanser Consulting, Inc.

[5] E. Kennedy and H. Tran, "Real-time implementation of a power series based nonlinear controller for the balance of a single inverted pendulum," in *Proceedings of The International MultiConference of Engineers and Computer Scientists 2015 Vol I, IMECS 2015*, Hong Kong, 18-20 March 2015, pp. 237–241, ISBN: 978–988–19 253–2–9, ISSN: 2078–0958 (Print); ISSN: 2078–0966 (Online).

[6] K. J. Astrom and K. Furuta, "Swinging up a pendulum by energy control," in *Prepints of the 13th IFAC World Congress*, vol. E, San Francisco, CA, 1996, pp. 37–42.

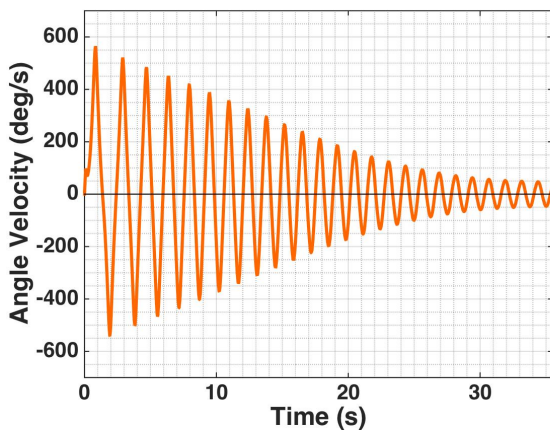[7] ——, "Swinging up a pendulum by energy control," *Automatica*, vol. 36, pp. 287–295, 2000.
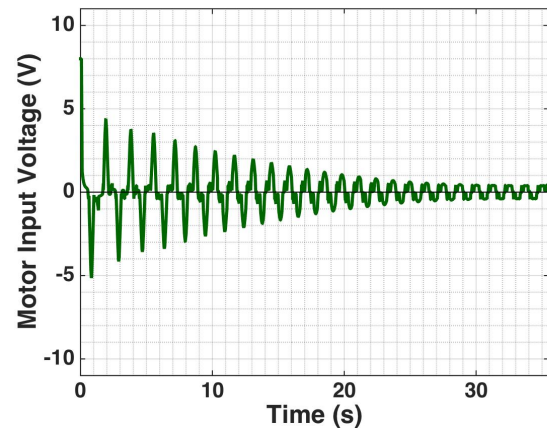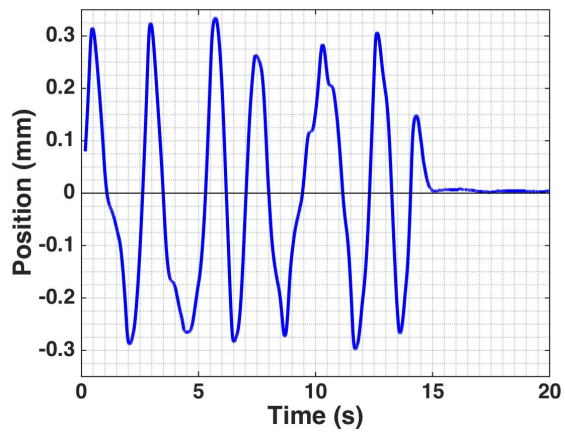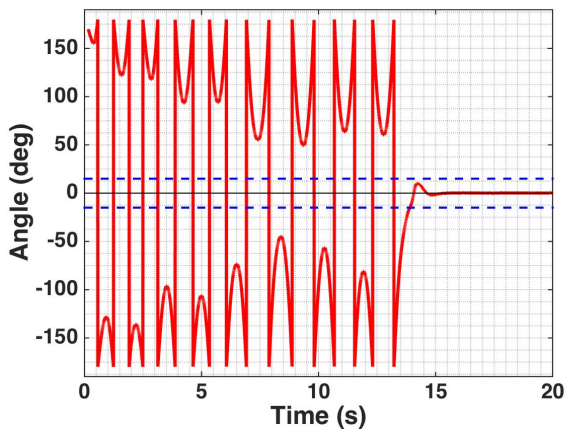
(a)

(b)

(c)

(d)

Fig. 5.   Simulated state response.
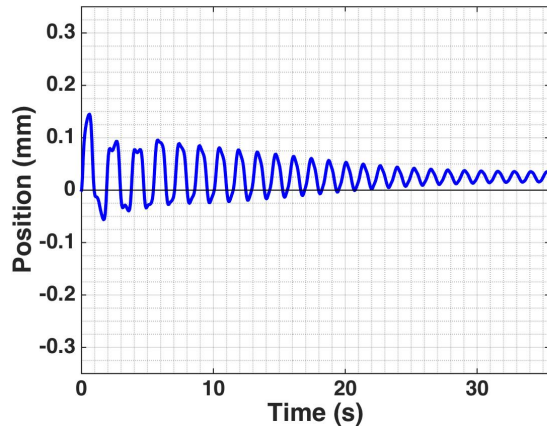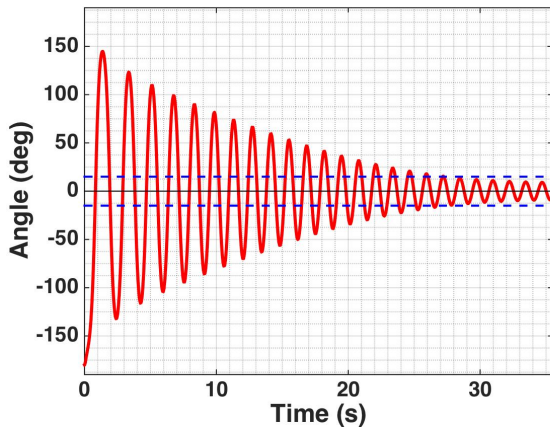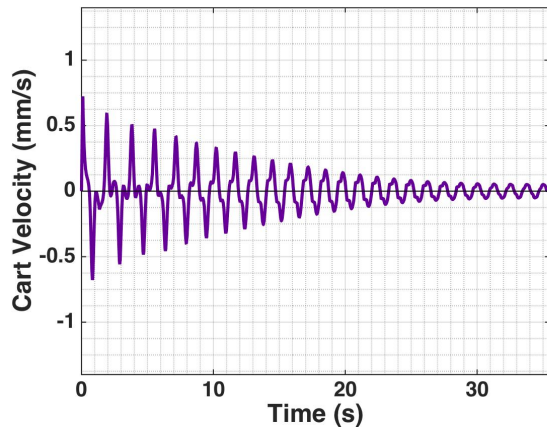
Fig. 6.   Simulated control effort.

(a)

(b)

(c)

(d)

Fig. 7.   Experimental state response.
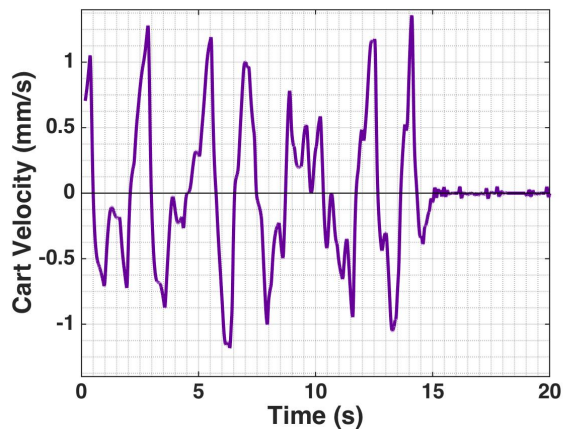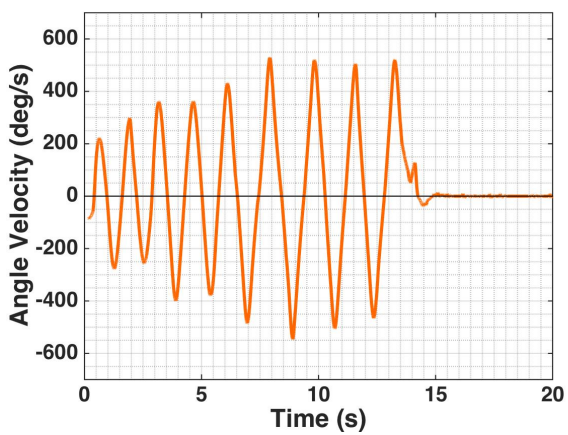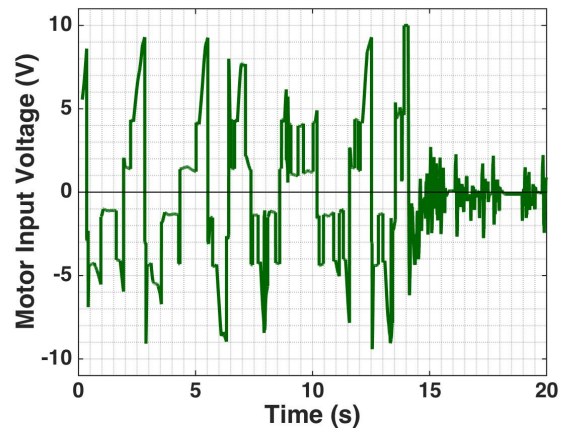
Fig. 8.   Experimental control effort.